Available online at www.sciencedirect.com

ScienceDirect

Procedia Manufacturing 34 (2019) 269–274

Procedia MANUFACTURING

www.elsevier.com/locate/procedia

47th SME North American Manufacturing Research Conference, Penn State Behrend Erie, Pennsylvania, 2019

# Effect of initial surface topography during laser polishing process: Statistical analysis

Evgueni Bordatchev[a,b,*,1], Srdjan Cvijanovic[b,a,1], O. Remus Tutunea-Fatan[b,a,*]

[a]National Research Council of Canada, London, Ontario, Canada, N6G 4X8
[b]Western University, London, Ontario, Canada, N6A 3K7

* Corresponding authors. Tel.: +1-226-688-5604; fax: +1-519-430-7064. *E-mail:* evgueni.bordatchev@nrc-cnrc.gc.ca / rtutunea@eng.uwo.ca; [1] first authors

**Abstract**

Surface finish is one of the most important quality characteristics of fabricated components. Laser polishing (LP) is one of the advanced manufacturing surface finishing techniques that has been recently developed and successfully employed for improving surface quality without deteriorating the overall structural form through surface smoothing by melting and redistributing a thin layer of molten material. This paper advances the statistical analysis of the LP process emphasizing aspects of the effect of the initial surface topography. Flat and ground initial surfaces are used for comparative statistical analysis of initial and polished profiles obtained experimentally. Their profile geometries and surface quality characteristics, such as, roughness, were compared and analyzed. In addition, LP process was experimentally investigated as a thermodynamic operator represented by a transfer function and it was examined by means of a coherence function.



*Keywords:* Laser polishing, surface quality, statistical analysis, initial topography, laser power, travel speed, roughness

## 1. Introduction

Laser polishing (LP) is one of the advanced manufacturing surface finishing techniques that has been continuously developed over the past two decades [1-6] and successfully employed for improving the surface morphologies of components made from various ferrous and non-ferrous materials. LP achieves good surface finishing without deteriorating the overall structural form through surface smoothing by melting and redistributing a thin layer of molten material over the surface through surface tension attempting to minimize surface energy. Since there is no material removal, the form of the given geometric feature is preserved. LP as one of the advanced manufacturing, knowledge-based technologies opens new avenues in cost effective manufacturing of value-added parts, components and tooling with complex 3D geometry eliminating manual or other types of finishing operations and significantly reducing overall tooling cost (up to 40%) and manufacturing time (up to 30%). The efficiency of LP technology is already proven since it has shown improvements of the surface quality as high as ~90% (from $S_a$ = 1.35 um before to $S_a$ = 0.18 um after LP, respectively) [7].

One of the main research and application challenges preventing the conversion of LP into a conventional technology is related to the lack of fundamental understanding on how the initial surface geometry influences the formation of LPed surface topography [8]. The team of researchers from Fraunhofer ILT has identified that one critical aspect of the LP

**Nomenclature**

| | |
|---|---|
| CF | coherence function |
| LP | laser polishing |
| TF | transfer function |
| $h_{ini}(x,y)$ | initial 2D surface topography |
| $h_{LP}(x,y)$ | LPed 2D surface topography |
| $R_a$ | profile average surface roughness |


10.1016/j.promfg.2019.06.150

process: LPed surface topography is formed by two processes – LP of the flat bulk material and LP of the initial surface topography (seen as deviations from the flat bulk material). In addition, two classes of the surface structures formed by the LP process were identified and thoroughly studied: a) surface structures produced by the dynamics of the melt and solidification front (ripples, undercuts), and b) surface structures produced by plastic deformation and changes in the microstructure (bulges, step structures, and martensite needles).

A different view on related aspects pertaining LP melting and redistribution was demonstrated in [9]: shallow surface melting (SSM) and surface over melting (SOM) effects were identified as dependent on the thickness of the melted layer. SSM regime was defined as being characterized by a melted layer thickness smaller than peak-to-valley distance such that molten peaks will flow down to valleys under the capillary pressure. This is also usually termed as capillary regime [10] in which high spatial frequencies are smoothed by surface tension and viscosity. When melted layer thickness is greater than the peak-to-valley distance, the SOM regime occurs and initial surface topography completely disappears. This case constitutes the so-called thermocapillary regime [10] according to which LPed topography with dominant low spatial frequency components is generated by high temperature gradients on the rapid solidification front. Despite the discrepant terminologies, the common and most critical conclusion of [8-10] is that these two regimes are typically lumped, in a sense that they take place simultaneously during LP. As a result, final Pled surface quality will be defined by the regime with a dominating performance. However, this also opens new opportunities in achieving best possible or desired surface quality through process parameters optimization aiming to control the effects of each regime.

In this context, the main objective of the current study was to demonstrate and characterize the differences in the surface topography formation having initial flat and ground surfaces for the same LP process parameters. Statistical modelling and analysis methodologies that were previously proposed [11] were utilized to separate the effects of the laser melting and solidification of both solid bulk material and initial surface topography. Several comprehensive statistical functions, such as transfer and coherence functions were employed to describe a statistical digital twin of the LP process and to demonstrate the dynamics of the LPed surface topography formation with respect to the laser power and travel speed and separate contributing surface formation processes. Overall, this manuscript aims to develop fundamental knowledge thorough understanding, and to establish additional engineering foundations of the LP technology by emphasizing aspects of surface quality characterization.

## 2. Statistical digital twin of the laser polishing process

Laser polishing (LP) process is a CNC-based technology where continuous or pulsed laser beam is travelling in accordance with a laser path trajectory for material melting, redistribution and solidification. Laser beam produces a continuous molten pool of the material moving it within prespecified area and smoothing the initial surface topography. The geometry and the volume of material polished depend on

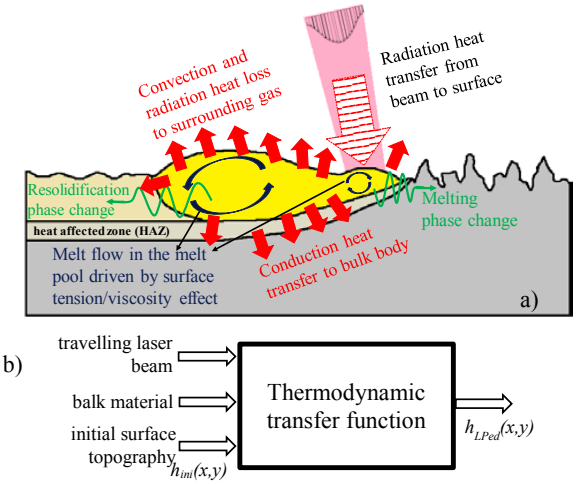


Fig. 1. Generalized schematics of the LP process (a) and its statistical digital twin (b).

the material properties and the laser-material interaction process parameters as related to laser, optics and motion. Fig. 1a shows the schematics of the LP process, which has a main functional goal to smooth the original surface geometry to a desired polished surface through laser-material interactions and by means of a set of process parameters related to machined material, laser, optics and laser beam motions.

Taking into account the main functional goal of LP to modify the geometry of original surface in order to achieve a better surface quality, LP process can be understood as a thermodynamic transformation of the original $h_{ini}(x,y)$ into the polished $h_{LP}(x,y)$ surface topography. It is common to represent surface geometry as a 1D (e.g., surface profile) or 2D (e.g., surface area) spatial random process, in which surface amplitude is a random variable of one, $h(x)$, or two, $h(x,y)$, surface coordinates, respectively. Therefore, by means of control theory and correlation/spectral analysis [12] of dynamic systems and LμP schematics as shown in Fig. 1b, LP process can be considered as a mathematical operator W(.) as a transfer function (TF). In spatial domain, this transformation can be described by the classical convolution integral surface geometry in 1D case for surface cross-sections [12]:

$$h_{LP}(\eta) = \int_{-\infty}^{+\infty} w(\eta) h_{ini}(x-\eta) d\eta \quad (1)$$

where $w(\eta)$ is the weighting function representing a statistical digital twin of the LP process in spatial domain. Fourier transformation of Eq. 1 produces a direct spatial frequency domain description of the LμP given as:

$$S_{LP}(\omega) = S_{ini}(\omega)\left|W(j\omega)\right|^2, \; S_{ini-LP}(j\omega) = S_{ini}(\omega)W(j\omega), \quad (2)$$

where $W(j\omega)$ is the transfer function of LP process; $S_{ini}(\omega)$, $S_{LP}(\omega)$ and $S_{ini\text{-}LP}(j\omega)$ are the autospectrums and cross-spectrum of original and polished surface profiles, respectively; $\omega$ is the spatial frequency, and $j=\sqrt{-1}$ is the imaginary unit.

The description presented above allows the understanding

and modelling LP process as a thermodynamic dynamic system including aspects of the laser-material interactions and physical-mechanical material properties. In this case, a complete description of LP process is only possible when both statistical characteristics of original and polished surfaces and dynamic characteristics of LμP process as a thermodynamic operator will be known and identified.

## 3. Experimental and surface analysis methodology

The experimental set-up for the LP process is shown in Fig. 2. The LP system is a complex opto-electro-mechanical CNC-controlled system and consists of a high-precision 3-axis motion system and a 1070 nm, 500 W continuous wave laser from IPG Photonics (model YLR-500). The motion system is controlled by a CNC motion controller from Aerotech with a position resolution of 0.1 μm such that accuracy and repeatability of laser beam motions was ensured. In addition, to allow highspeed 2D scanning within 100 x 100 mm working envelope, the laser beam was directed to a 2-axis galvanometric scanning head, manufactured by ScanLab and with an f-theta objective having a focal length of 160 mm. Laser focal position was defined through single spot tests.

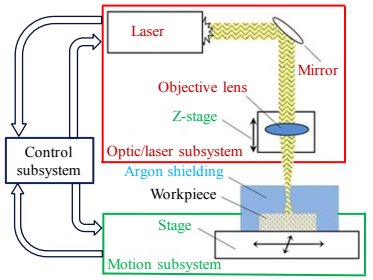


Fig. 2. Generalized schematic of the LP system.

The surface topography analysis methodology consisted of three primary steps: a) measurement of original surface geometry $h_{ini}(x,y)$ between alignment marks, b) performing LP experiments on previously measured surface, and c) measurement of LPed surface geometry $h_{LP}(x,y)$ using marks for alignment with respect to the original surface profile. The sample surfaces before and after polishing were measured using a WYKO NT1100 white light interferometer, having a 1Å height measurement resolution. The pixel resolution of the surface scan was 0.258 μm, and auto-stitching technique was applied to increase the measuring envelope. Digitized $h_{ini}(x)$ and $h_{LP}(x)$ were used for calculating two critical statistical characteristics, e.g. transfer (TF) and coherence (CF) functions [12], for comprehensive description of the surface topography thermodynamic transformation during LP process.

Two sets of LP experiments were performed on H13 tooling steel samples varying laser power from 25 W to 100 W and travel speed from 250 mm/s to 1000 mm/s. Most critical and unique aspects of these LP experiments are that two H13 samples have significantly different initial surface topography: ground and perfectly flat shown in Figs. 3 and 4, respectively. This selection represents the primary focus of this study, namely to statistically analyze the effect of initial surface topography on LP process in order to enhance its digital twin.

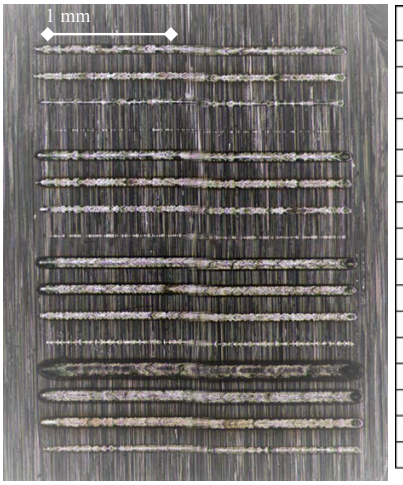


| power W | speed mm/s |
|---|---|
| 100 | 1000 |
| 75 | |
| 50 | |
| 25 | |
| 100 | 750 |
| 75 | |
| 50 | |
| 25 | |
| 100 | 500 |
| 75 | |
| 50 | |
| 25 | |
| 100 | 250 |
| 75 | |
| 50 | |
| 25 | |

Fig. 3. LPed sample with ground initial surface.

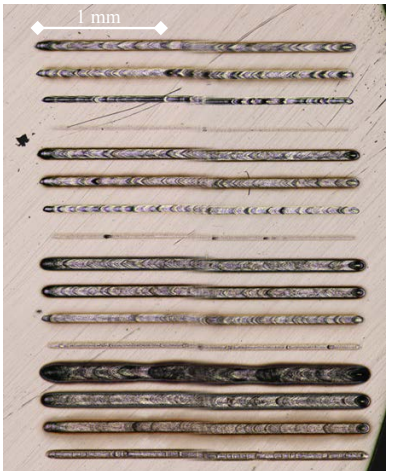


| power W | speed mm/s |
|---|---|
| 100 | 1000 |
| 75 | |
| 50 | |
| 25 | |
| 100 | 750 |
| 75 | |
| 50 | |
| 25 | |
| 100 | 500 |
| 75 | |
| 50 | |
| 25 | |
| 100 | 250 |
| 75 | |
| 50 | |
| 25 | |

Fig. 4. LPed sample with initially flat surface.

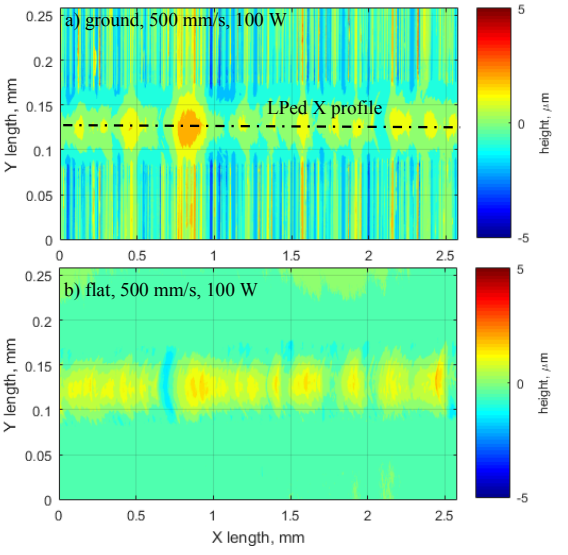


Fig. 5. Typical 3D topography of ground and flat surfaces.

Ground initial surface represents a variety of spatial frequencies of the topography having a profile average roughness $R_a$ = 0.75…0.98 µm. Initial surface of a flat sample was machined by single point diamond cutting and yielded $R_a$ = ~0.033 µm over the entire area. Typical 3D topographies of ground and flat initial surfaces with examples of LPed lines are shown in Fig. 5. LPed lines were produced with a length of 3 mm, however only central 2.5 mm length was used for statistical analysis where steady state LP takes place. For this feasibility study, only notable dissimilar pairs of LP process parameters were selected from the range of performed experiments in order to differentiate the effects of laser power and travel speed on surface topography formation. Thus, LP experiments performed with a laser power of 25 W and 100 W and with a travel speed of 500 mm/s were used for analysis of the laser power effect and experiments performed with a travel speed of 250 mm/s and 750 mm/s and with a laser power of 75 W were used for analysis of the travel speed effect.

## 4. Surface topology characterization of LPed samples with initially ground surface

Effect of the laser power on ground initial surface topography was studied by comparing initial and LPed profiles $h_{ini}(x)$ and $h_{LP}(x)$ and statistical interdependence characteristics between them, such as TF and CF. Fig. 6 shows comparative analysis of the ground initial and LPed profiles. The focus of this analysis is on how LP with different levels of laser power changes thermodynamic self-organizational distribution of the molten material in longitudinal direction under dynamic surface tension and capillary flow. However, it should be kept in mind that these are only specific cases drawn from a more complex 3D thermo-dynamic phenomenon [7]. Several other important observations can also be drawn from this analysis. Firstly, laser power critically contributes to the effectiveness of the LP process as 34.6% was achieved for a laser power of 25 W at 500 mm/s travel speed reducing $R_a$ from 0.746 µm to 0.488 µm (see Fig. 6a) as LP with a laser power of 100 W reduced $R_a$ from 0.801 µm to 0.510 µm (see Fig. 6b) gaining very similar 36.3% surface quality improvement. However, the areal distributions of the molten material are completely different for these two cases. Low-power LP is smoothing surface profile very lightly and thus acts as a statistical moving averaging of the surface profile. This can be confirmed by a calculated mean value for both ground and flat initial profiles – -0.031 µm and 0.376 µm, respectively. As such, the bulging effect lifts initial surface profile by 0.407 µm. However, for the higher level of power, LPed surface profile was moved up by 1.204 µm. In this case, the bulging effect is three times smaller and acts as an amplitude modulator for the initial profile.

Such observations can be supported by the comparative analysis of the TF and CF shown in Figs. 7 and 8, respectively. It is evident, that $TF_{25\,W}$ and $CF_{25\,W}$ have much wider width than $TF_{100\,W}$ and $TF_{100\,W}$ meaning that linear thermo-dynamic transformation of the initial into LPed profiles occurs in this range of the spatial frequencies. Both LP processes with low (25 W) and high (100 W) laser power perform as expected as a low-pass filter [10, 11], however, with different cut-off frequencies. It also can be observed that $LP_{100\,W}$ amplifies low-frequency components more than $LP_{25\,W}$ up to a spatial

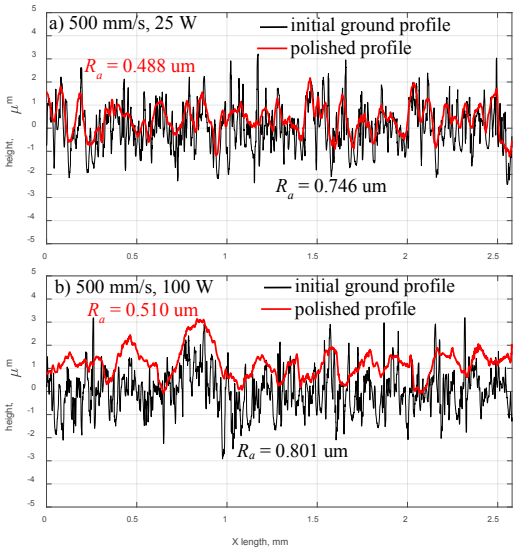


Fig. 6. Effect of the laser power on ground surface topography.

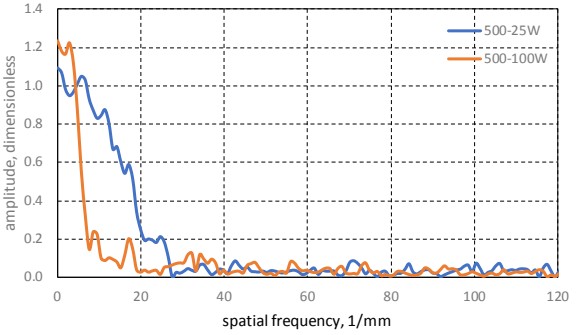


Fig. 7. Transfer function of ground surfaces LPed with 25 W and 100 W.

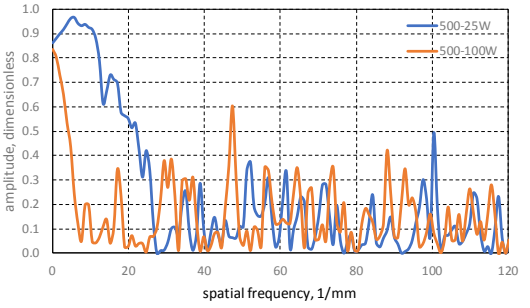


Fig. 8. Coherence function of ground surfaces LPed with 25 W and 100 W.

frequency of ~5 $mm^{-1}$, while $TF_{25\,W}$ gradually reduces amplitudes of the initial profile frequency components. It is known [12] that linear dynamic models can be applied only when CF > 0.7…0.8, and therefore statistical digital twin can be applied for the surface profile transformation preferably for the low laser power LP process. $LP_{100\,W}$ has statistical correlation with initial surface profile only in a waviness range (e.g. up to 1.25 $mm^{-1}$ for a cut-off length of 0.8 mm per ISO 4288). Therefore, classic thermodynamic LP models may be only applied for surface profile and waviness formations.

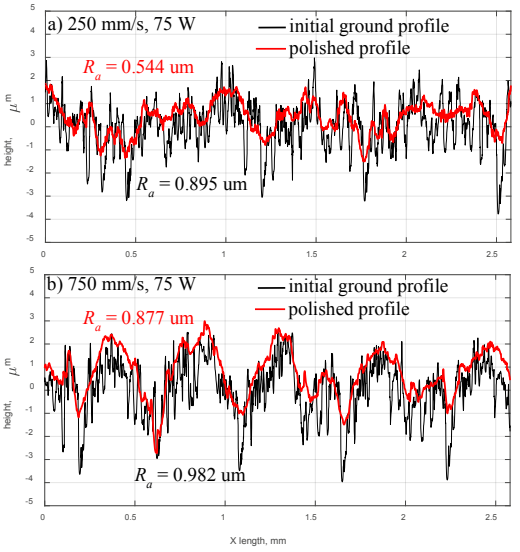


Fig. 9. Effect of the travel speed on ground surface topography.

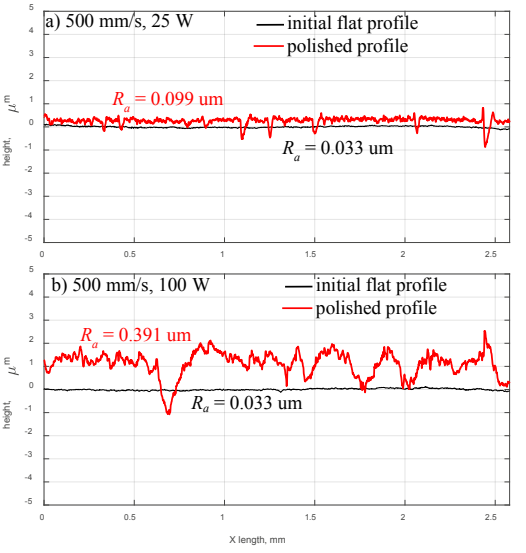


Fig. 12. Effect of the laser power on flat surface topography.

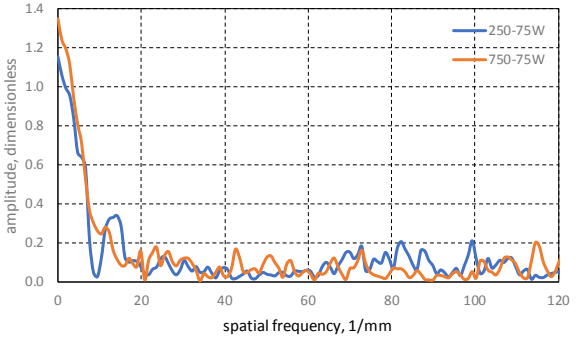


Fig. 10. Transfer function of ground surfaces LPed with 250 and 750 mm/s.

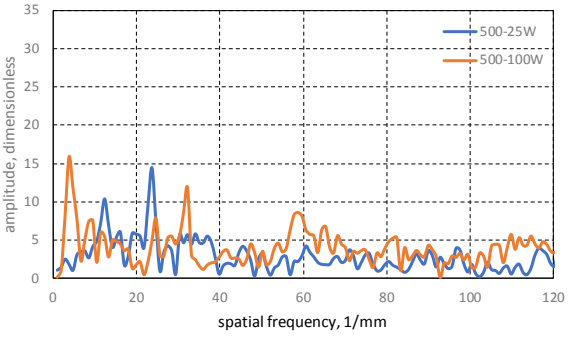


Fig. 13. Transfer function of flat surfaces LPed with 25 W and 100 W.

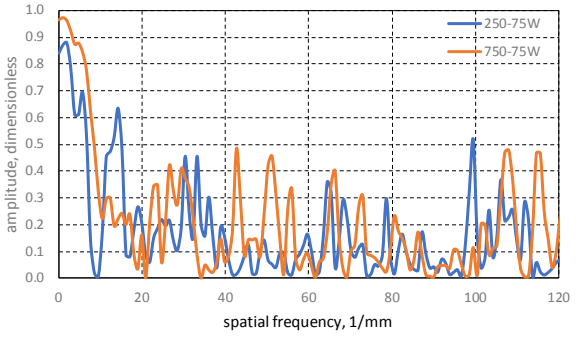


Fig. 11. Coherence function of ground surfaces LPed with 250 & 750 mm/s.

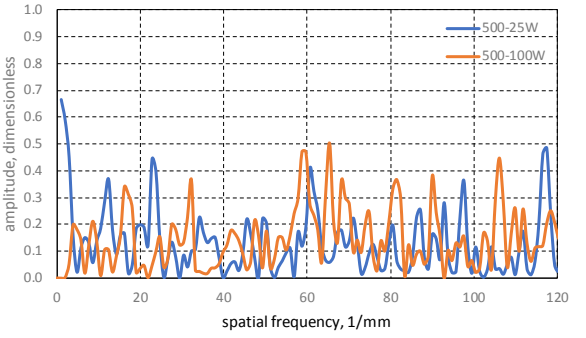


Fig. 14. Coherence function of flat surfaces LPed with 25 W and 100 W.

The effect of the travel speed on ground initial surface topography is shown in Figs. 9-11. The comparison of initial and LPed profiles $h_{ini}(x)$ and $h_{LP}(x)$ (see Fig. 9) demonstrates an effect similar to laser power effect according to which low travel speed LP acts as a moving average and smooths mainly high frequency components. This is also confirmed by $TF_{250}$ and $TF_{750}$ (see Fig. 10) and $CF_{250}$ and $CF_{750}$ (see Fig. 11) having a similar cut-off frequency ~7 $mm^{-1}$ whereas $TF_{750}$ amplifies waviness components more than $TF_{250}$.

## 5. Surface topology characterization of LPed samples with initially flat surface

The analysis of the 3D topography formation on flat initial surface represents a pure thermodynamic effect of the LP process on a bulk material since surface topography variations are below 30 nm. Such LP experiments can be also used for the verification of thermodynamic modelling with initially flat surfaces [7].

The effect of the laser power on flat initial topography is shown in Figs. 12. The comparison of initial and LPed profiles for $LP_{25\ W}$ and $LP_{100\ W}$ demonstrates that significant variations in the LPed topography occur even at low laser power due to the bulk material-laser interactions resulting in forming bulging geometry of the laser track. It was found that the mean value for the $LP_{25\ W}$ was -0.029 µm and 0.263 µm for $LP_{100\ W}$. Thus, the bulging effect lifts the initial profile by 0.292 µm. However, for the higher level of power, LPed profile was moved up by 0.882 µm. These values of the bulging effect are somewhat lower than for the ground initial surface. An additional possible reason for the lower bulging values can reside in a higher reflectance value of the flat initial surface. The analysis of the TF and CF shown in Fig. 13 and 14, respectively, does not uncover any statistically meaningful information since there is no formation of the periodical structures in the LPed profiles. This result was expected as bulk material-laser interactions are predominantly a non-linear thermodynamic process with self-organization of the LPed topography due to the surface tension, molten material flow viscosity, and capillary effects.

The effect of the travel speed on flat initial topography is shown in Fig. 15. Travel speed seems to have a smaller impact of the formation of LPed topography than laser power. This observation is based on the fact that for significantly different travel speeds (250 mm/s and 750 mm/s) $R_a$ values of LPed lines are very similar, e.g. 0.342 µm and 0.323 µm, respectively. In contrast, laser powers of 25 W and 100 W, yield $R_a$ values of 0.099 µm and 0.391 µm, respectively (see Fig. 12).

## 5. Summary and conclusions

This study presents an advanced statistical analysis of the LP process that emphasizes the effect of initial surface topography. Flat and ground initial surfaces were used for comparative statistical analysis of initial and polished profiles obtained experimentally. Profile geometries and surface quality characteristics, e.g., roughness, were compared and analyzed. In addition, LP process was experimentally assimilated with a thermodynamic operator represented by a transfer function and it was examined by means a coherence function. The following conclusions can be drawn from the results above:

- LP is a complex physical-thermo-dynamic process, in which in addition to laser, optics, material, and motion related parameters, original surface geometry also plays a critical role on the formation of the polished surface.
- Formation of the LPed surface topography includes a bulging effect and involves two major processes: bulk material-laser interactions and an additional effect from the non-uniform initial surface.
- Contributions brought by the two processes are not linear and smoothing a given material and initial surface can be only achieved when the effect of the polishing process itself on the bulk material will be as minimal as possible.
- Travel speed affects roughness of the LPed lines significantly more than laser power.
- Future research and full analysis of the performed LP experiments will need to continue the development of fundamental/engineering foundation for the LP technology.

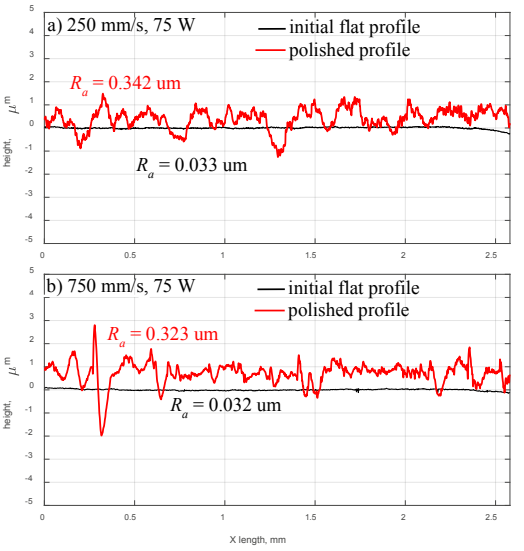


Fig. 15. Effect of the travel speed on flat surface topography.

## Acknowledgements

This study is the result of collaboration between the National Research Council of Canada (London, Ontario) and Western University (London, Ontario). Partial financial support was also provided by the Natural Sciences and Engineering Research Council (NSERC) of Canada.

## References

[1] Willenborg E. Polieren von werkzeugstählen mit laserstrahlung, Dissertation RWTH Aachen, Shaker Verlag Aachen 2006
[2] Willenborg E. Polishing with laser radiation. In: Poprawe R, editor: Tailored Light 2: Laser Allication Technology., 2011. P. 196-202
[3] Temmler A, Willenborg E, Wissenbach K. Laser polishing. Proceedings of SPIE 8243: paper 82430W, 13 p.
[4] Pfefferkorn FE, Duffie NA, Li X, Vadali M, Ma C. Improving surface finish in pulsed laser micro polishing using thermocapillary flow. CIRP Annals - Manufacturing Technology 2013; 62:203–206
[5] Pfefferkorn FE and Morrow JD. Controlling surface topography using pulsed laser microstructuring. CIRP Annals-Manuf Tec 2017; 66:241-244
[6] Bordatchev EV, Hafiz AMK, Tutunea-Fatan OR. Performance of laser polishing in finishing of metallic surfaces. Int J Adv Manuf Technol 2014; 73:35–52
[7] Mohajerani S, Bordatchev EV, Tutunea-Fatan RO. Recent developments in modeling of laser polishing of metallic materials. Lasers in Manuf and Materials Processing, published on-line 28 Sept 2018; 35 p.
[8] Nusser C, Kumstel J, Kiedrowski T, Diatlov A, and Willenborg E. Process- and material-induced surface structures during laser polishing. Advanced Engineering Materials 2015; 3:268-277
[9] Ukar E, Lamikiz A, López de Lacalle LN, del Pozo D, Arana JL. Laser polishing of tool steel with $CO_2$ laser and high-power diode laser. Int J Mach Tool Manuf 2010; 50:115–125
[10] Pf efferkorn, F.E., Duffie, N.A., Li, X., Vadali, M., Ma, C. (2013). Improving surface finish in pulsed laser micro polishing using thermocapillary flow. CIRP Annals – Manuf Tech, 62, 203-206
[11] Chow MTC, Hafiz AMK, Tutunea-Fatan OR, Knopf GK, Bordatchev EV. Experimental statistical analysis of laser micropolishing process. In: Proceedings of the International Symposium on Optomechatronic Technologies (ISOT) 2010, Toronto, Canada, 6 pp.
[12] Bendat JS and Piersol AG. Engineering applications of correlation and spectral analysis, John Wiley & Sons, New York NY USA, 1993